Heliyon 10 (2024) e36719

Contents lists available at ScienceDirect

Heliyon

journal homepage: www.cell.com/heliyon

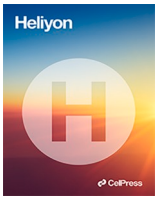

Research article

Experimental study on the impact of indoor unit airflow velocity on the performance of an automotive heat pump system with a suction line heat exchanger

Alpaslan Alkan

Department of Mechanical Engineering, Sakarya University of Applied Sciences, Sakarya, 54187, Turkey

ARTICLE INFO

Keywords:
Heat pump
Automobile
Heat exchanger
R1234yf
R134a
Exergy

ABSTRACT

This study aimed to investigate the effect of changing the indoor unit air flow rate on the performance of an automobile heat pump with a suction line heat exchanger. Using a four-way valve, the automotive heat pump system was developed by reversing the refrigerant direction in the automobile air conditioning system, excluding the compressor. A suction line heat exchanger was added to the test system to enhance heat transfer between the liquid and suction lines of the automotive heat pump system. Performance comparisons were first performed for R134a and R1234yf by disabling the suction line heat exchanger. Then, the suction line heat exchanger was activated for R1234yf, and the tests were repeated. Performance comparisons were made for two different compressor speeds and three different indoor unit airflow speeds. It was found that using the heat exchanger in R1234yf operations improved the heating capacity, compressor discharge temperature and coefficient of performance by approximately 1.8 %, 5.1 % and 5.9 %, respectively. The heating capacity of the heat pump system using R134a, R1234yf, and R1234yf with the suction line heat exchanger was determined to be in the range of 2.46–3.29 kW, 2.35–3.04 kW, and 2.39–3.11 kW, respectively. An increase in the airflow speed of the indoor unit from 1.4 m s^{-1} to 3.2 m s^{-1} resulted in an average decrease of approximately 12.3 % in the compressor discharge temperature. In contrast, the heating capacity and coefficient of performance increased by approximately 11.8 % and 14.4 % on average, respectively, for R1234yf operations with the heat exchanger. This study revealed that by optimizing the air flow rate in the R1234yf heat pump system with a suction line heat exchanger, improvements in the heating capacity and coefficient of performance can be achieved, thus providing better thermal comfort in the passenger compartment.

1. Introduction

Industrialisation was among the most rapid developments during the last century. Industrialisation led to an increase in the use of unnatural working fluids, which led to environmental problems. The most significant environmental problem is the loss of the atmospheric ozone layer and the high penetration of ultraviolet rays. Another significant environmental problem is global warming. The refrigerants used in automobile air conditioning (AAC) systems contribute to these environmental problems. The use of R12 refrigerant, a chlorofluorocarbon (CFC) compound used in AAC systems, was limited by the Montreal Protocol in 1987 due to the destruction

E-mail address: aalkan@subu.edu.tr.

https://doi.org/10.1016/j.heliyon.2024.e36719
Received 25 April 2024; Received in revised form 8 July 2024; Accepted 21 August 2024
Available online 25 August 2024

of the ozone layer by the chlorine atom included in the refrigerant [1]. The industry adopted R134a, a hydrofluorocarbon (HFC) compound, as a substitute for R12. The Kyoto Protocol has imposed gradual restrictions on the use of R134a due to its significant global warming potential (GWP) [2]. An F-gas regulation followed this protocol requiring that starting in 2017, AAC systems in the European Union could use refrigerants with a GWP value of up to 150 [3]. These environmental regulations were accelerated studies on alternative refrigerants. Leading environment-friendly alternative refrigerants include CO_2 (R744), R152a, R1234yf and R1234ze (E). Due to the supercritical operation of R744, the effective pressures of the AAC system using R744 are about seven times as high as the pressures of the R134a system [4]. Thus, the burst strength of the R744 AAC system components should be 7–10 times higher when compared to R134a, which leads to lower heat transfer due to the higher component weight and wall thickness in the heat exchanger. The R152a refrigerant, which has A2 flammable properties, could not be used in AAC systems [5]. R1234yf refrigerant is in the A2L group, which is slightly flammable, has a GWP of 4, is compatible with the R134a AAC system with minor modifications, and could be used as an alternative refrigerant to replace R134a [6].

There are many studies in the literature on the use of R1234yf instead of R134a in AAC systems. These studies generally show that the use of R1234yf in AAC systems with R134a reduces system performance [7–12]. In the literature, studies on suction line heat exchangers (SLHX), which provide heat exchange between the evaporator outlet suction line and the condenser outlet liquid line, investigate how the SLHX could perform to reduce this loss. Cho and Park [13] conducted a study to evaluate and compare the efficiency and effectiveness of R1234yf and R134a refrigerants in an AAC system that includes an SLHX. They found that the R1234yf system had 4.0–7.0 % lower cooling capacity and 3.6–4.5 % lower COP compared to the R134a system. However, they stated that the R1234yf system showed almost equivalent cooling capacity to the R134a system when the SLHX was added. They showed that the COP of the R1234yf system with the SLHX was 0.3–2.9 % lower than the R134a system for the compressor speeds between 800 and 1800 rpm, but 0.9 % higher when the compressor speed increased to 2500 rpm. They stated that the second law efficiency of the R1234yf system was 3.4–4.6 % lower than the R134a system at all compressor speeds but improved by 1.5–4.6 % with the addition of the SLHX. Prabakaran et al. [14] studied a performance evaluation between R1234yf and R134a refrigerants in the AAC system. They accomplished this by including an SLHX. Based on their report, the optimal quantities of refrigerant for the system were determined to be 740g for R134a and 670g for R1234yf. They argued that the AAC system, which included the SLHX, an optimal thermostatic expansion valve (TXV), and R1234yf, could replace AAC systems that utilized R134a. Prabakaran et al. [15] conducted a study on the thermodynamic performance and environmental impact of an AAC system with an SLHX using R134a and R1234yf. They stated that R1234yf performed better than R134a at low compressor speeds in the AAC system with an SLHX, regardless of the evaporator inlet air flow rate, temperature and condenser inlet air speed. However, they showed that R1234yf performed slightly worse at medium and higher compressor speeds. They observed an increase in COP, exergy efficiency, and cooling capacity with the increase in evaporator inlet air flow rate, temperature, and condenser inlet air flow rate. They suggested that the performance degradation in the system with R1234yf at medium and higher compressor speeds may be due to increased power consumption and poor cooling capacity. Gungor and Hosoz [16] investigated the effect of using an SLHX on the performance of an R1234yf and R134a AAC system with an orifice tube as an expansion device. They found that the cooling capacity of the AAC system with R1234yf was 6.9 % higher and 22.5 % lower than the AAC system with R134a, depending on the use and absence of an SLHX, respectively. They stated that the COP of the AAC system with R1234yf without SLHX and with SLHX was 10.9 % and 3.5 % lower than the AAC system with R134a, respectively. They observed that the exergetic efficiency of the R1234yf AAC system without SLHX and with SLHX was 41.5 % and 8.4 % lower than the AAC system with R134a, respectively. They showed that the use of SLHX in the AAC system with R1234yf compensates for the lack of cooling capacity compared to the AAC system with R134a and that the AAC system with R1234yf has higher performance than the AAC system with R134a.

Today, electric motor vehicles increasingly replace conventional automobiles powered by internal combustion engines. However, electric vehicles, like internal combustion engine vehicles, lack a heat source to warm the passenger cabin in cold conditions. Electric vehicles also require a heat source to warm the battery to a certain temperature during cold days. Thus, electric vehicles require an automobile heat pump (AHP) to heat the passenger cabin and the battery for initial start-up in cold weather [4,17]. An AAC system could be used as an AHP by changing the compressor inlet and outlet refrigerant flow direction with a four-way valve. Then, the evaporator would function as a condenser and the condenser would function as an evaporator. Heating is achieved by drawing the heat from the low-temperature heat source and releasing heat into the indoor environment. Hosoz and Direk [18] established an R134a AHP system and conducted heating and cooling experimentally. They declared that the heating efficiency of the system was adequate at about 10 °C or above. They reported that the AHP heating COP was higher than the AAC cooling COP. Hosoz et al. [19] developed an R134a AHP system specifically designed for a diesel car. The researchers examined the steady-state and transient performances of the AHP system using several sources of heat, including ambient air, engine coolant, and exhaust gas. The researchers discovered that the engine coolant caused the highest heating capacity and COP, whereas ambient air resulted in the lowest values. Wang et al. [20] conducted an empirical investigation to evaluate the efficiency of R134a and R407C refrigerants in an AHP system for an electric car operating in low ambient air conditions. The R407C AHP system demonstrated superior heating capacity and compression power compared to the R134a AHP system. Nevertheless, the former had a lower COP. Wang et al. [21] investigated the performance of a R744 AHP system under various cold climate conditions. They recorded a COP of 3.1 and a heating capacity of 3.6 kW at outside and interior temperatures of −20 °C. Zou et al. [22] designed an R1234yf AHP system with a secondary refrigerant cycle to reduce high-voltage power requirements for heating electric vehicles. They demonstrated that the heating performance was significantly affected by the expansion valve and operating conditions. Wang et al. [23] reported that when the outdoor temperature was −20 °C, the R744 AHP system could achieve 1.8 COP and 5.6 kW maximum heating capacity, which were more efficient when compared to traditional positive temperature coefficient (PTC) heaters. Direk and Yuksel [24] experimentally investigated R1234ze(E), R152a, and R444a as R134a alternatives in an AHP system. Their study showed that R152a had a greater heating capacity than R134a, R444a, and

R1234ze(E). Additionally, increasing the overall compressor volume might enhance the heating capacity of R1234ze(E). Zhang et al. [25] showed an exergy analysis on an electric vehicle AAC-AHP system with a thermal battery management system. Under AAC-AHP operating circumstances, the compressor was identified as the primary cause of exergy loss in the system. They confirmed that the heating efficiency of the AAC-AHP system was more efficient when compared to PTC heating. Direk and Yuksel [26] reported the performances of both refrigerants based on different performance parameters in AAC-AHP systems with R134a and R1234yf. Their experimental findings demonstrated that although the cooling and heating capacity and COP of the R1234yf were lower than R134a, R1234yf could be used in both AAC and AHP systems due to its environment-friendly properties. Aral et al. [27] developed an experimental AAC-AHP system with R134a and R1234yf refrigerants. They tested the cooling and heating performance of the system under various compressor speeds and temperatures. They determined that the heating performance of the R1234yf system was better when compared to the cooling performance and exhibited slightly lower energy efficiency. Alkan et al. [28] researched the performances of R134a and R1234yf AHP systems. They reported that the COP and heating capacity of the R1234yf were between 1.6 – 7.1 % and 9.2–15.4 %, respectively, based on various conditions and lower when compared to those of the R134a. Huang et al. [29] demonstrated the feasibility and superiority of the R290 refrigerant-based water cycle electric vehicle heat pump air conditioning system through the establishment of a performance test platform. Their experimental findings demonstrated that the system's cooling capacity at a high temperature of 55 °C was 5.05 times greater. On the other hand, the isentropic efficiency of the system in the heating mode at a low temperature of −20 °C exceeded 80 %. Lei et al. [30] investigated the exergy analysis of low GWP alternative refrigerants R1234yf, R152a and R744 for AHP systems used in all-electric vehicles (EVs) by modelling. They determined that R1234yf and R152a refrigerants exhibited similar performance to R134a, while R744 refrigerant showed lower efficiency. They found that reducing indoor and outdoor airflow and compressor speed could increase the efficiency of R1234yf and R152a systems, while increasing the condenser airflow for the R744 system could be beneficial. They also stated that reducing the compressor speed and ambient temperature and increasing the condenser airflow would increase the efficiency of R1234yf, R152a and R744 systems. Song et al. [31] evaluated the performance of R290 and R744 refrigerants as an alternative to R1234yf in electric vehicle heat pump systems and their performance under extreme operating conditions. They stated that R744 refrigerant cannot be used in R1234yf systems due to its high thermodynamic operating pressure range. On the other hand, they demonstrated that R290 can be partially substituted in R1234yf systems because it has similar properties. They observed that the heating and cooling capacities of the R290 system were 158 % and 112 % higher, respectively, than the R1234yf system. They stated that the COP of the R290 system in heating and cooling modes was 84 % and 83 % higher, respectively than the R1234yf system. Tasdemirci et al. [32] performed the performance evaluation of an experimental AHP system using R134a and R1234yf with and without an SLHX. They found that the R1234yf system with SLHX provided an average of 13.9 % lower heating capacity but 7.8 % higher COP with respect to total power consumption compared to the

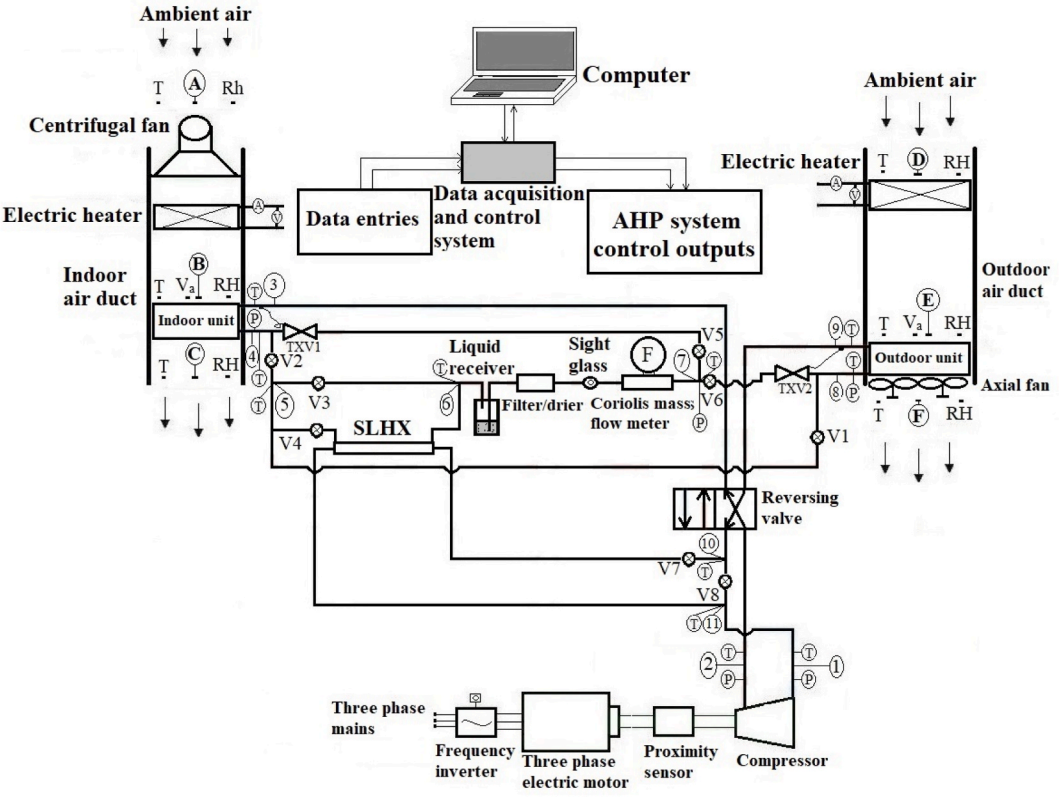

Fig. 1. The schematic diagram of the experimental AHP system with the SLHX.

R134a system. They also found that the R1234yf system with SLHX had an average of 22.3 % lower exergy destruction rate per unit heating capacity compared to the R134a system.

This study deals with improving the performance of the AHP system, which has become an important issue in electric vehicles that are becoming increasingly widespread today. Studies in the literature investigated the performance of R1234yf in AAC systems. In addition, studies have aimed to enhance the performance of R1234yf in AAC systems by adding extra equipment such as SLHX or by improving the existing system components. However, in these studies, performance analyses were performed as a function of only a few parameters. Furthermore, the comparisons of the effect of indoor unit air flow rate, which is an important factor in achieving thermal comfort in the cabin, on the performance are only made for certain compressor speeds. This study aims to reveal how the performance of the R1234yf AHP system with and without an SLHX changes as a function of the compressor speed and indoor unit airflow velocity by performing energy and exergy analyses. In addition, by using R134a in the AHP system, performance comparisons of both refrigerants were made for the same operation conditions.

2. The experimental apparatus and methodology

Fig. 1 illustrates the schematic representation of the experimental AHP incorporating SLHX. The system was implemented by adding an SLHX and a four-way valve to an AAC system. In the AHP system, an SLHX was placed between the liquid line at the indoor unit outlet and the suction line at the outdoor unit outlet. The AHP system had a fixed-capacity seven-cylinder wobbling plate compressor, an evaporator (laminated indoor unit), a condenser (outdoor unit with parallel flow microchannel), a liquid tank, a filter/dryer, two TXVs, an SLHX, and eight manual valves shown by the letter V in Fig. 1. The technical specifications of the system components are shown in Table 1.

In the AHP system, a three-phase asynchronous 5.5 kW electric motor connected to the 380 V AC electricity mains through a frequency inverter was used to provide the desired compressor speed. This electric motor was connected to the compressor with the help of a belt-pulley mechanism. The original evaporator in the AAC system was mounted on the indoor unit air duct, and the condenser was mounted in the outdoor unit air duct. The ducts were 100 cm long and fit the size of the heat exchangers mounted in the outdoor and indoor air ducts. 5.4 and 1.8 kW electric heaters were mounted in the outdoor and indoor air ducts, respectively, to obtain the desired airflow temperatures at the inlets of the outdoor and indoor units. Twin axial fans were placed at the entrance of the outdoor unit, which yielded a maximum airflow speed of 3.6 m s^{-1} in the outdoor unit air duct. On the other hand, a centrifugal fan providing a maximum airflow of 3.4 m s^{-1} was mounted at the entrance of the indoor unit air duct.

The experimental system is equipped with mechanical measuring devices for relative humidity, temperature, pressure, refrigerant mass flow rate, airflow speed and compressor speed measurements required to calculate the performance parameters and control the desired experimental conditions at the points shown in Fig. 1. The refrigerant mass flow rate was measured using the Coriolis mass flow meter installed on the liquid line outlet of the liquid tank. The pressure transmitters and Bourdon manometers were used to measure the inlet and exit pressures of the compressor. The pressures were also measured at the exit of the indoor unit, inlet of the outdoor unit, and the liquid line of the cooling cycle using pressure transducers placed, as indicated by P in Fig. 1. T-type thermocouples were used to measure refrigerant temperatures at various locations throughout the cooling cycle, as indicated by the letter T in Fig. 1.

The relative humidity, dry bulb temperature, and airflow velocity measurements were carried out to determine the thermodynamic properties of the air passing over the indoor and outdoor units. In addition, the airflow velocity and dry bulb temperature data were used to control the airflow temperature and velocity. The relative humidity and dry bulb temperature of the air streams were measured using SHT 71 humidity and temperature sensors. The measurements were taken from certain points of the indoor and outdoor air ducts, indicated by T and RH, as seen in Fig. 1. These points were selected as the places where the average temperature data were obtained. The airflow velocities passing through the indoor and outdoor air ducts were measured with airflow transmitters placed at the inlet of the indoor and outdoor heat exchangers, indicated by Va in Fig. 1. These points were selected as the places where the average airflow velocity was obtained.

All sensor data in the AHP system were collected with data acquisition cards and transferred to the computer using the MODBUS communication protocol defined as RS485. Some of these data were used instantly for the control of the experimental system. According to the experimental comparison parameters, the compressor speed of the system, the temperatures and the speeds of the indoor and outdoor unit's air flow were conditioned according to the experimental conditions with various control systems. The desired

Table 1
Technical details of the components of the experimental AHP.

Component	Description
Compressor	Type: seven-cylinder fixed capacity Stroke volume: 154.90 cc/rev
Outdoor unit	Type: Parallel flow microchannel Sizes: 63 cm × 38 cm × 2 cm
Indoor unit	Type: laminated Sizes: 23.5 cm × 22 cm × 6.5 cm
Expansion valves	Type: internally equalised thermostatic expansion valves Capacity: 5.5 kW
SLHX	Type: Coaxial (tube-in-tube) Dimensions: 29.85 cm (Length)

compressor speed was conditioned with a PLC-controlled inverter electric motor using the data obtained from the proximity sensor used to measure the compressor speed in Fig. 1. The indoor and outdoor unit airflow inlet temperatures were kept at the desired values by using PLC-controlled current switches that activate and deactivate the electrical resistances of the electric heaters to obtain the desired temperature. DC driver cards that control the fan motors per the desired airflow rate based on the airflow data coming from the airflow transmitters located at the unit inlets provide the conditioning of the indoor and outdoor unit airflow rates. The measurement device specifications are presented in Table 2. The general view of the AHP system and the assembly view of the SLHX are presented in Fig. 2.

Table 3 provides various properties of R134a and R1234yf refrigerants used in the AHP system. These refrigerants are non-toxic, pure, and have an ODP of zero. The centennial GWP of the R134a was 1430, and it did not comply with the EU F-gas regulation. R1234yf is an unsaturated organic composite comprised of carbon, fluorine, and hydrogen, its centennial GWP was 4, and it was classified by ASHRAE as a slightly flammable (A2L) refrigerant [2]. Although R1234yf is corrosive with atmospheric oxidation of trifluoroacetic acid, it was not considered dangerous since the carbon-fluorine bond is consistent [33]. Since R1234yf's atmospheric residence is short (11 days), it quickly disappears into the atmosphere. While the liquid density of R134a is greater than that of R1234yf, its vapour density is lower.

Initial experiments were conducted by charging 2000 g of R134a to the AHP system. Before the experiments with R1234yf, R134a was recovered from the system, and 1800 g of R1234yf was charged into the system. According to Cho et al. [35], the system required 10 % less R1234yf owing to its liquid density being roughly 10 % lower than that of R134a.

The AHP systems were evaluated under three different indoor unit airflow velocities and two compressor speeds. The indoor unit airflow rate was determined as three different speed values to provide low, medium and high speeds as the indoor cabin air flow rates in an automobile air conditioning system. The indoor unit inlet airflow velocities were measured to be 1.4, 2.4, and 3.2 m s^{-1}. The outdoor unit inlet airflow velocity was measured to be 3.5 m s^{-1}. Compressor speeds were conventionally determined as 1000 and 2000 rpm, which are the average idling and operating speeds of the internal combustion engine, respectively. As previously mentioned, the compressor drive was provided by a three-phase asynchronous electric motor. The airflow temperatures at the inlets of the indoor and outdoor units were kept constant at 5 °C. Furthermore, the relative humidity of the air that entered both the outdoor and interior units was consistently maintained within a range of 70 ± 10 %. The tests were terminated when the data obtained from the system became stable for 3-5 minutes at specified test conditions. The steady-state operation was usually attained in 10–15 min once the AHP system was turned on. Steady-state data were obtained by calculating the average of the data collected in the last 3–5 min of the tests.

3. Thermodynamic analysis of the experimental AHP

The concept of energy conservation was utilized to examine the energy performance characteristics of the experimental AHP components. This analysis assumed that there were no pressure decreases in the refrigeration cycle lines as well as in the indoor and outdoor units. Additionally, it was assumed that the kinetic and potential energy changes in the components are negligible.

The heating capacity of the system may be calculated by applying the principle of conservation of energy to the indoor unit [9]:

$$\dot{Q}_{iu} = \dot{m}_r(h_3 - h_4) \tag{1}$$

The refrigerant mass flow rate, denoted as $\dot{m}_r$, and the enthalpy of the refrigerant, denoted as h, can be determined using REFPROP 9.1 software [34] as a function of pressure and temperature.

The amount of power supplied to the refrigerant in the adiabatic compressor may be calculated using the following equation [9]:

$$\dot{W}_{comp} = \dot{m}_r(h_2 - h_1) \tag{2}$$

The COP is a measure of the energy efficiency of the AHP and is calculated by dividing the heating capacity by the compressor power [9].

$$COP = \frac{\dot{Q}_{iu}}{\dot{W}_{comp}} \tag{3}$$

The application of the exergy balance equation to system components could be used to determine their thermodynamic inefficiencies. For control volumes, this equation could be written as follows [36,37]:

Table 2
Specifications of the measurement devices.

Physical measure	Apparatus	Variety	Uncertainty
Temperature of refrigerant	Type T thermocouple	−40 - 350 °C	±0.5 °C
Temperature of air dry bulb	SHT-71	−40 - 123 °C	±0.4 °C
Pressure	Vika S−10 transmitter	0–25 bar	±0.25 bar
Relative humidity	SHT-71	0–100 %	±3 %
Air velocity	(EE65−VCK200) transmitter	0.2–10 m s^{-1}	±0.2 m s^{-1}
Mass flow rate	Krohne Optimass 3300C H04 (Coriolis flow meter)	0–450 kg h^{-1}	±0.1 %

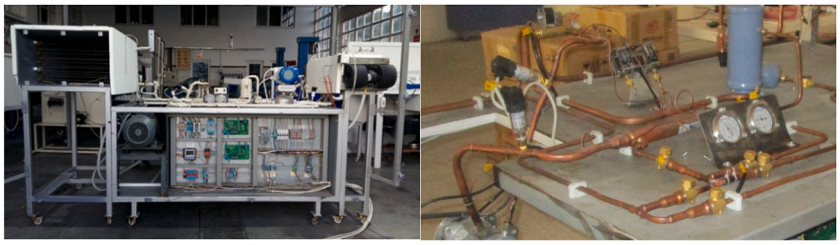

(a) (b)

Fig. 2. Picture of the experimental AHP; (a) General view, (b) View of the SLHX assembly.

Table 3
Various specifications of R134a and R1234yf [28,34].

Refrigerant	R134a	R1234yf
Chemical formula	CH_2FCF_3	$C_3H_2F_4$
Molecular mass (g mol^{-1})	102.03	114.04
Point of boiling (°C)	−26.3	−30
Critical temperature (°C)	101.1	94.7
Critical pressure (kPa)	4059.3	3382.2
Density of liquid at 0 °C (kg m^{-3})	1294.8	1176.3
Vapour density at 0 °C (kg m^{-3})	14.428	17.647
Ozone-depleting potential	0	0
Global-warming potential	1430	4
ASHRAE Safety Group	A1	A2L

$$\sum\left(1-\frac{T_0}{T_j}\right)\dot{Q}_j-\dot{W}_{cv}+\sum\dot{m}_{in}\psi_{in}-\sum\dot{m}_{out}\psi_{out}=\dot{E}x_d \tag{4}$$

In this equation, T_0 represents the temperature of the surrounding environment, T_j represents the temperature at the boundary, $\dot{Q}_j$ denotes the rate at which heat is transferred at the boundary, $\dot{W}_{cv}$ means the work output of the control volume, $\dot{m}$ represents the rate at which mass flows, ψ denotes the specific flow exergy, and $\dot{E}x_d$ means the rate at which exergy is destroyed within the control volume. The equation for determining the specific flow exergy of the refrigerant is [9]:

$$\psi=(h-h_0)-T_0(s-s_0) \tag{5}$$

Where the subindex "0″ represents the system in a non-functional state, specifically under normal environmental circumstances. The specific airflow energies at points B, C, and E shown in Fig. 1 were determined from Refs. [18,38].

$$\psi_a=\left(c_{p,a}+\omega\,c_{p,v}\right)T_0\left[\left(\frac{T}{T_0}\right)-1-ln\left(\frac{T}{T_0}\right)\right]+\left[(1+1.6078\,\omega)R_aT_0\,ln\left(\frac{P}{P_0}\right)\right]$$
$$+R_aT_0\left\{(1+1.6078\,\omega)\,ln\left(\frac{1+1.6078\,\omega_0}{1+1.6078\,\omega}\right)+1.6078\,\omega\,ln\left(\frac{\omega}{\omega_0}\right)\right\} \tag{6}$$

In this equation, $c_{p,v}$ and $c_{p,a}$ represent the specific heat of water vapour and air, R_a is the ideal gas constant for dry air, ω is the specific humidity, and P denotes the pressure. The exergy destruction rates for the components of the AAC system were calculated using Equation (4). The resulting equations for the components are shown in Table 4, where $\dot{m}_{a,ou}$ and $\dot{m}_{a,iu}$, represent the rates at which air mass flows through outdoor and indoor units, respectively.

The exergy destruction in the reversing valve may be disregarded due to the effective insulation of the component and the little heat transfer between the two streams passing through it. The total exergy destruction in the AHP system can be calculated from

Table 4
The exergy destructions in the components of the AHP system.

Component	Equation
Compressor	$\dot{E}x_{d,comp}=\dot{m}_r(\psi_{comp,in}-\psi_{comp,out})+\dot{W}_{comp}$
Outdoor unit	$\dot{E}x_{d,cond}=\dot{m}_r(\psi_{ou,in}-\psi_{ou,out})+\dot{m}_{a,ou}(\psi_E-\psi_F)$
Expansion valve	$\dot{E}x_{d,TXV}=\dot{m}_r(\psi_{TXV,in}-\psi_{TXV,out})$
Indoor unit	$\dot{E}x_{d,evap}=\dot{m}_r(\psi_{iu,in}-\psi_{iu,out})+\dot{m}_{a,iu}(\psi_B-\psi_C)$
SLHX	$\dot{E}x_{d,SLHX}=\dot{m}_r(\psi_{SLHX,in}-\psi_{SLHX,out})$

$$\dot{E}x_{d,tot} = \dot{E}x_{d,comp} + \dot{E}x_{d,ou} + \dot{E}x_{d,TXV} + \dot{E}x_{d,iu} + \dot{E}x_{d,SLHX} \quad (7)$$

4. Uncertainty analysis

The Moffat [39] technique was used to evaluate the uncertainty in the individual performance parameters of the AHP system. According to this technique, the uncertainty of a y function consisting of n measurable variables, namely x_1, x_2, …, x_n, can be determined from

$$u_y = \sqrt{\sum_{i=1}^{n} \left(\frac{\partial y}{\partial x_i} u_{x_i} \right)^2} \quad (8)$$

where, u_{x_i} indicates the uncertainty of the measured variable i.

Consequently, the maximum uncertainties for heating capacity, compression power, and COP were determined as 0.0355 kW, 0.0385 kW, and 0.0258, respectively, based on the experimental data and the accuracy of the devices presented in Table 2.

5. Results and discussion

Comparisons of the performance parameters of the AHP system with R1234yf and R134a and the effect of the SLHX on them in the R1234yf system are exhibited in Fig. 3–11 as a function of indoor unit air face velocity and compressor speed. The indoor and outdoor unit inlet air temperatures in these figures are 5 °C. Furthermore, the outdoor unit inlet air speed is 3.5 m s^{-1}. In Fig. 3 – 10, three different indoor unit inlet air speeds of 1.4, 2.4, and 3.2 m s^{-1} and two different compressor speeds of 1000 and 2000 rpm were used. The P – h and T – s graphs in Fig. 11 are presented for the indoor unit air speed of 2.4 m s^{-1} and compressor speed of 2000 rpm.

The variations in conditioned air temperature exiting from the AHP system indoor unit are presented in Fig. 3. When the compressor speed was 1000 rpm, it was observed that the indoor unit air outlet temperatures of the AHP system using R134a, R1234yf, and R1234yf with SLHX increased by 15.91, 10.81, and 12.87 °C, respectively as the indoor unit air face velocity decreased from 3.2 to 1.4 m s^{-1}. When the compressor speed was 2000 rpm, it was observed that the indoor unit air outlet temperatures of the AHP system using R134a, R1234yf, and R1234yf with SLHX increased by 14.71, 16.64, and 17.86 °C as the indoor unit air face velocity decreased from 3.2 to 1.4 m s^{-1}. As the refrigerant saturation temperature increased with the decrease in the indoor unit airflow rate and the increase in the indoor unit refrigerant pressure, the difference between the refrigerant and airflow temperatures increased. Thus, the indoor unit outlet temperature increased. The AHP system utilizing R1234yf exhibited a decrease in indoor unit air outlet temperature of approximately 5.06 °C compared to the AHP system using R134a. However, this difference reduced to about 3.39 °C when the SLHX was activated in the AHP system with R1234yf. The results of this study show that, as in the AHP studies in the literature, the temperature of the indoor unit outlet air is higher in the R134a system than in the R1234yf system [27,28]. However, according to the results obtained from this study, it is seen that this range can be reduced by adding an SLHX to the R1234yf system. In addition, reducing the indoor unit airflow speed to the optimum will increase the airflow temperature, thus providing better thermal comfort in the vehicle cabin.

The changes in refrigerant mass flow rate of the AHP systems as a function of indoor unit air velocity are presented in Fig. 4. It was observed that the refrigerant mass flow rate increased by 11.1 %, 4.5 %, and 4.9 % in the AHP system using R134a, R1234yf, and R1234yf with SLHX, respectively, together with the increase in indoor unit air face velocity from 1.4 to 3.2 m s^{-1} for both compressor speeds. R1234yf had a higher flow rate since its vapour density was 22.3 % higher when compared to the R134a refrigerant at the same saturation temperature. The experiments demonstrated that the refrigerant mass flow rate was 22.6 % and 21.7 % higher in the R1234yf AHP system with disabled and operated SLHX in comparison to the AHP system with R134a. These results show that R1234yf

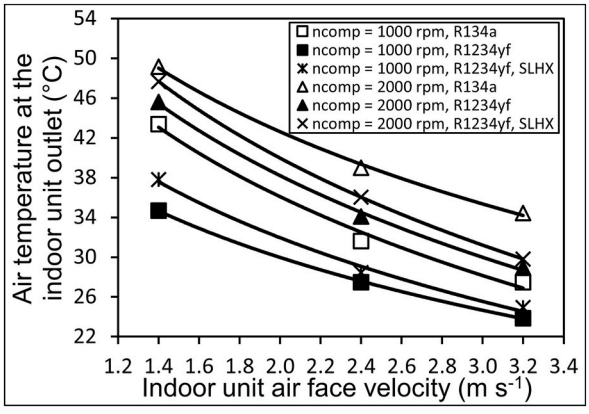

Fig. 3. The relationship between the air temperature at the outlet of the indoor unit and the air face velocity of the indoor unit.

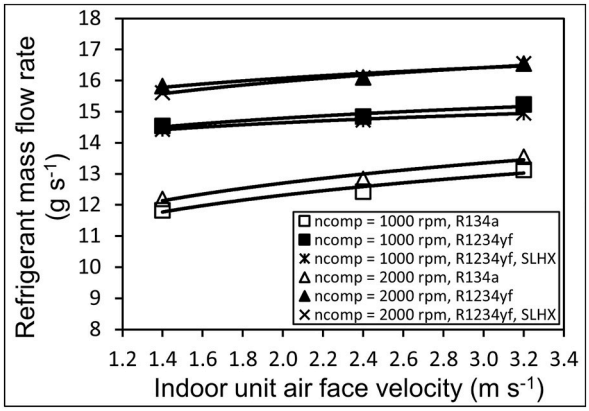

Fig. 4. The relationship between the mass flow rate of the refrigerant and the air face velocity of the indoor unit.

has a higher refrigerant mass flow rate than R134a, which is in agreement with the literature [15,27]. There is a slight decrease in refrigerant mass flow rate with the addition of SLHX in the R1234yf system as found in Refs. [13,35]. It has been observed that the refrigerant mass flow rate increases due to the increase in heat transfer in the indoor unit with the increase in the indoor unit air flow rate.

The variations in AHP system heating capacity are presented in Fig. 5 as a function of the indoor unit air speed. As the indoor unit air flow rate rises, the heating capacity increases due to the refrigerant mass flow rate increment. The heating capacity of the AHP system using R134a, R1234yf, and R1234yf with SLHX increased by 12.5 %, 11.6 % and 11.1 %, respectively, when the indoor unit air face velocity increased from 1.4 to 3.2 m s^{-1} for both compressor speeds. The experimental findings demonstrated that the heating capacity of the AHP system using R134a, R1234yf, and R1234yf with SLHX was 3.28 kW, 3.04 kW, and 3.11 kW, respectively, at 2000 rpm compressor speed and 3.2 m s^{-1} indoor unit air face velocity. The heating capacity of the R1234yf system was enhanced by 1.8 % when the SLHX was activated. It was observed in the literature that the R1234yf AHP system had a lower heating capacity than the R134a AHP system [27,28]. However, in this study, it has been found that adding the SLHX to the R1234yf AHP system can improve the heating capacity. Increasing the indoor unit air flow rate causes an increase in the heating capacity. However, as seen in Fig. 3, increasing the indoor unit air flow rate causes a decrease in the indoor unit outlet air temperature. The most suitable cabin thermal comfort according to various conditions can be provided with the indoor unit air flow rate, where the indoor unit outlet air temperature and heating capacity are optimum. The findings of the study can be used to attain the desirable cabin thermal comfort conditions in a short period by providing more suitable indoor air outlet air temperature and heating capacity by changing the indoor unit air flow rate.

The variations in compressor power of the AHP systems are presented in Fig. 6 as a function of the indoor unit air speed. It was observed that the compressor power increased by 7.5 %, 7.7 %, and 5.9 %, respectively, in the AHP system using R134a, R1234yf, and R1234yf with SLHX via the increase in the indoor unit air face velocity from 1.4 to 3.2 m s^{-1} for the compressor speed of 1000 rpm. However, the compressor power decreased by 2.4 %, 0.8 %, and 3.9 %, respectively, in the AHP system using R134a, R1234yf, and R1234yf with SLHX with the increase in the indoor unit air face velocity from 1.4 to 3.2 m s^{-1} for the compressor speed of 2000 rpm. The increase in the compressor speed increased the compressor power due to the rise in the refrigerant mass flow rate and the compression ratio. It was observed that the compressor power was in the range of 0.55–0.97 kW, 0.54–0.91 kW, and 0.53–0.87 kW,

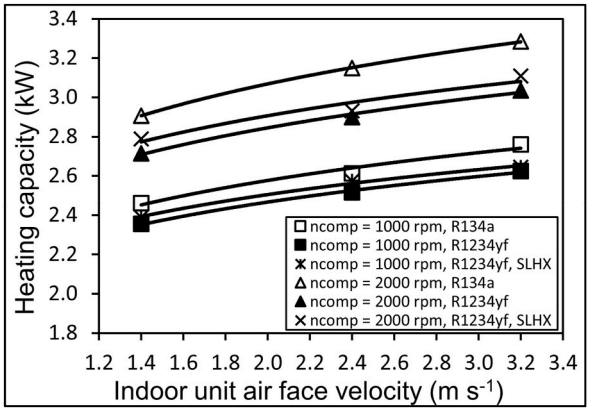

Fig. 5. The heating capacity as a function of the indoor unit air face velocity.

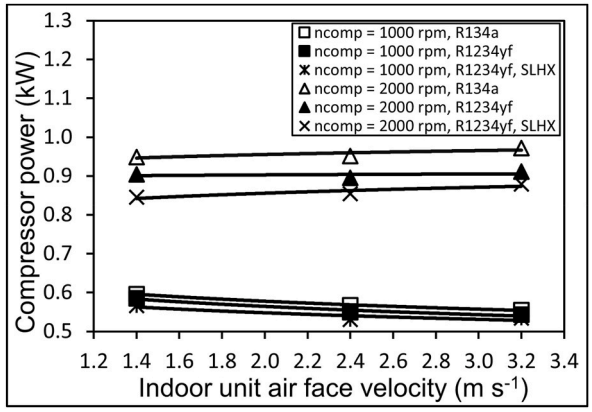

Fig. 6. The compressor power as a function of the indoor unit air face velocity.

respectively, in the AHP system using R134a, R1234yf, and R1234yf with SLHX. It was determined that the compressor power was reduced by approximately 3.8 % in the R1234yf AHP system with SLHX. The reduction in compressor power can be ascribed to the decrease in the pressure ratio across the compressor, which originated from the increase in the compressor inlet pressure due to the use of the SLHX. In addition, since the SLHX added to the R1234yf AHP system caused a slight decrease in the refrigerant flow rate as seen in Fig. 4, there was also a slight decrease in the compressor power. In the literature [13,16,26,28], it is generally reported that the compressor power increased with the increase in the compressor speed. In this study, it is seen that the compressor power increases especially with the increase in the compressor speed and also with the increase in the indoor unit air flow rate [15].

The variations in COP of the AHP system are presented in Fig. 7 as a function of the indoor unit air speed. For both refrigerants, COP increased with the increase in the indoor unit air speed and decreased with the rise in the compressor speed. It was observed that the COP increased by 15.4 %, 15.7 %, and 12.2 %, respectively, in the AHP system using R134a, R1234yf, and R1234yf with SLHX when the indoor unit airflow face velocity was increased from 1.4 to 3.2 m s^{-1} for both compression speeds. It was determined that the addition of SLHX to the R1234yf AHP system led to a 5.9 % increase in the COP. COP reveals the energy effectiveness of the system as it gives the heating capacity per unit compressor power. It has been observed in agreement with the literature that as the compressor speed increases, the COP decreases due to the faster increase in the compressor power in comparison to the heating capacity [13,15,26,28]. It has been observed that the COP increases with the increase in indoor unit air flow rate due to the faster increase in the heating capacity compared to the compressor power This situation also was reported in literature studies carried out with evaporator air flow rates in the AAC systems [15]. Literature reveals that cooling/heating capacities and COPs of R1234yf AAC/AHP systems are generally lower than R134a systems [7,16,28]. There are also some studies showing that R1234yf gives better results than R134a under certain conditions [15]. In this study, when the SLHX was added to the R1234yf AHP system, an increase in the COP was observed due to the decrease in compressor power as seen in Fig. 6 and the increase in the heating capacity as seen in Fig. 5.

The variations in the compressor discharge temperature are reported in Fig. 8 as a function of the indoor unit air speed. It was determined that the compressor discharge temperature increased with the increase in the compressor speed; however, it decreased with the increase in the indoor unit airflow face velocity. The increase in the compressor speed increased the discharge pressure and refrigerant mass flow rate, thus leading to an increase in the compressor discharge temperature. The increase in the indoor unit airflow face velocity increased the heat transfer between the refrigerant and the air. Thus, the compressor discharge temperature decreased

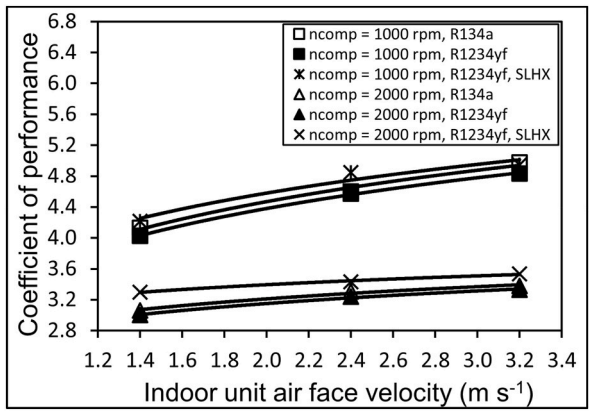

Fig. 7. The COP as a function of the indoor unit air face velocity.

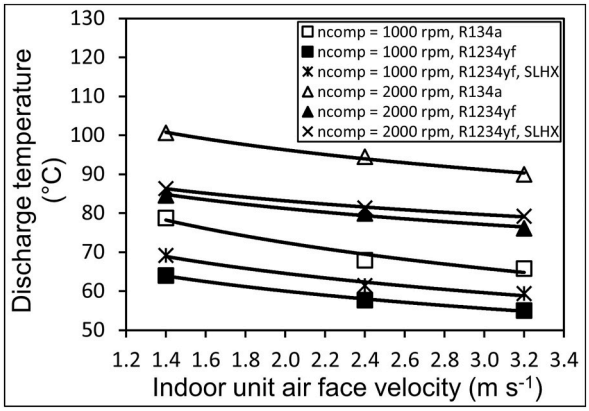

Fig. 8. The compressor discharge temperature as a function of the indoor unit air face velocity.

due to the decrease in the indoor unit pressure and the refrigerant saturation temperature. High discharge temperatures deteriorate the compressor lubrication oil, shortening the life of the compressor. However, it increases the heating capacity since it promotes heat rejection to the conditioned air stream in the indoor unit. It was observed that the AHP system using R134a exhibited higher compressor discharge temperatures in the range of 10.26–16.01 °C, and 6.36–14.22 °C, respectively, when compared to the AHP system using R1234yf, and R1234yf with SLHX. It was observed that the addition of the SLHX to the R1234yf AHP system increased the compressor discharge temperature by 5.1 %. In both AAC and AHP studies in the literature [16,27,28,35], it was reported that the compressor discharge temperature increased with increasing compressor speed. Furthermore, in the studies conducted on AAC systems [16,35], it was stated that the SLHX added to the system increased the compressor discharge temperature.

Exergy destruction in the components of the AHP system is presented in Fig. 9 for the compressor speeds of 1000 and 2000 rpm at 3.2 m s^{-1} indoor unit airflow velocity. In all experiments, the outdoor unit had the highest exergy destruction. The outdoor unit exhibited the greatest exergy destruction at the compressor speed of 1000 rpm, followed by the indoor unit, compressor, and TXV. Similarly, the outdoor unit exhibited the greatest exergy destruction at the compressor speed of 2000 rpm, followed by the indoor unit, compressor, and TXV. Exergy destruction in the indoor and outdoor units was mostly due to the increase in heat transfer by the temperature difference between the refrigerant and the air streams. When the compressor speed was increased from 1000 rpm to 2000 rpm, the exergy destruction in the indoor unit increased by 20.7 %, 23.7 % and 17.2 %, respectively, in the AHP system using R134a, R1234yf, and R1234yf with the SLHX. It was observed that the addition of the SLHX to the R1234yf AHP system reduced the exergy destruction in the indoor unit by 16.4 %. It can be observed in Fig. 8 that the compressor discharge temperature in the R134a system was higher when compared to the R1234yf system. Thus, the exergy destruction in the indoor unit was 7.7 % and 23.8 % higher in the AHP system using R134a when compared to the AHP system using R1234yf and R1234yf with SLHX, respectively. It was determined that the exergy destruction was 15.7 % and 19.1 % higher in the outdoor unit of the AHP system using R1234yf and R1234yf with SLHX compared to the AHP system using R134a, respectively. The exergy destruction was 16.5 % and 50.2 % higher in the compressor of the AHP system using R1234yf and R1234yf with SLHX when compared to the AHP system using R134a, respectively. The exergy destruction was 83.1 % and 62.1 % higher in the TXV of the AHP system using R1234yf and R1234yf with SLHX compared to the AHP system using R134a, respectively. Although the compressor pressure was lower in R1234yf when compared to R134a, the exergy destruction was higher in the compressor, TXV and outdoor unit due to the higher refrigerant mass flow rate. Furthermore, the increase in the refrigerant mass flow rate, compressor pressure, and compressor discharge temperature with increasing compressor speed led to higher exergy destruction in all components [28]. Similar results were obtained in the literature regarding the increase in the exergy destructions in the components of the AHP and AAC systems with increasing compressor speed [13,28]. In addition, it has been stated in the literature that the addition of the SLHX to the AAC system using R1234yf decreased the exergy destroyed in the evaporator and TXV, while the exergy destroyed in the compressor and condenser increased [13]. In this study, it has been observed that the use of SLHX in the R1234yf AHP system decreases the exergy destroyed in the indoor unit and TXV, while increasing the exergy destroyed in the outdoor unit and compressor.

Fig. 10 illustrates the variations in the exergy destruction per unit heating capacity of the AHP system as a function of the indoor unit airflow speed. If the increase in the total exergy destruction rate in all AHP systems is greater than the increase in heating capacity, it increases the total exergy destruction rate per unit heating capacity in AHP systems. This occurs when the speed of the compressor rises or when the airflow rate of the indoor unit decreases. Moreover, when the compressor speed increases, the pressure in the compressor also increases, resulting in a drop in the evaporation temperature of the outdoor unit and an increase in the condensation temperature of the indoor unit. In this case, the temperature difference between the airflow temperature passing through the outer surface of the heat exchangers and the refrigerant passing through the inner surface increases. Furthermore, a rise in pressure resulted in a corresponding rise in exergy destruction in both the compressor and TXV. In comparison to the AHP system with R134a, the exergy destruction per unit heating capacity in the AHP system using R1234yf and R1234yf with SLHX was determined to be 20.1 % and 22.2 % higher, respectively. The rise in the airflow velocity of the indoor unit from 1.4 to 3.2 m s^{-1} resulted in a reduction in the total exergy destruction per unit heating capacity in the AHP system using R134a, R1234yf, and R1234yf with SLHX by 16.7 %, 12.7 %, and 11.8 %

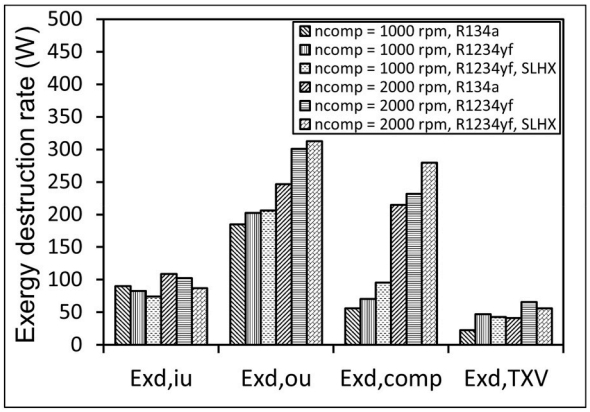

Fig. 9. The exergy destruction rates in the components of the AHP system.

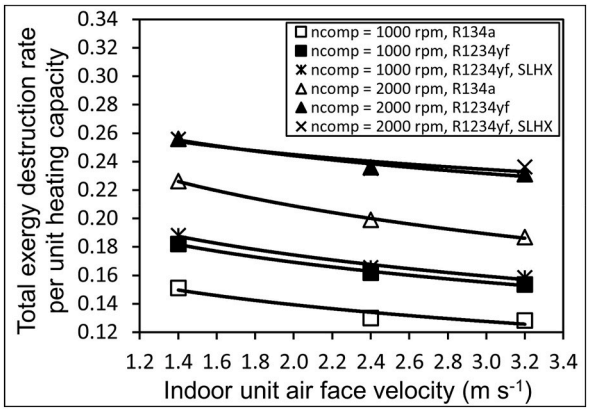

Fig. 10. The rate of exergy destruction per unit heating capacity as a function of the indoor unit air face velocity.

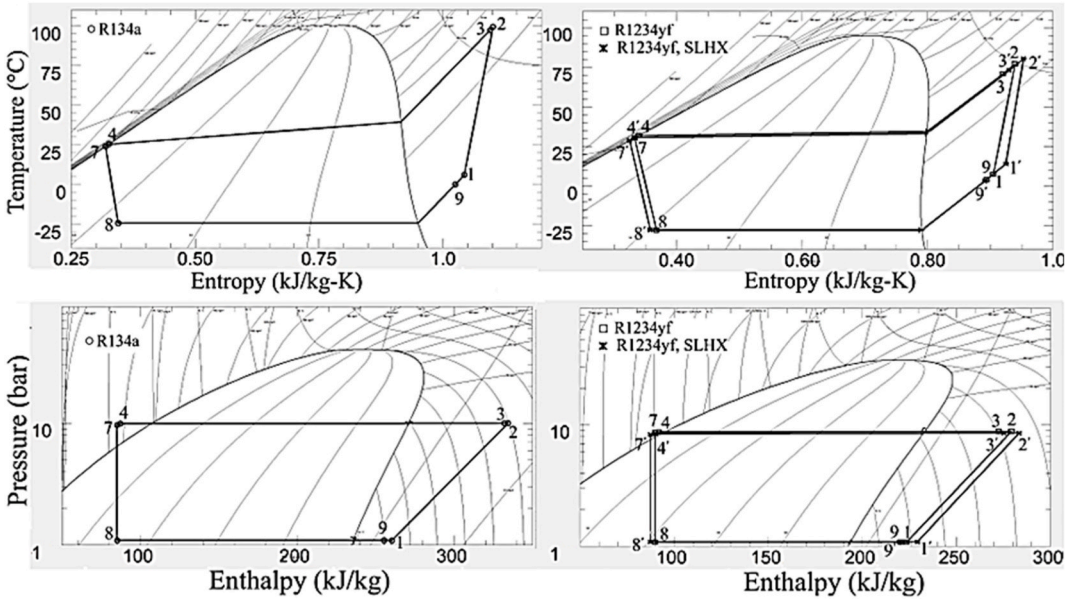

Fig. 11. Representation of T-s and P-h diagrams of the cycle for an experimental condition.

respectively. According to the literature, in both AAC and AHP systems, the total exergy destruction per unit heating capacity increased as the compressor speed increased [28,32]. Adding an SLHX to the AHP system caused a slight increase in the total exergy destruction per unit heating capacity. However, increasing the indoor unit air flow rate can reduce the total exergy destruction per unit heating capacity.

Fig. 11 shows the T-s and P-h diagrams of AHP systems using R134a, R1234yf, and R1234yf with the SLHX for the compressor speed of 2000 rpm, indoor unit inlet airflow velocity of 2.4 m $s^{-1,}$ and outdoor unit airflow velocity of 3.5 m s^{-1}. The locations of the points are shown in Fig. 1. The line $\overline{12}$ shows the work absorption in the compressor, $\overline{34}$ indicates the heat rejection in the indoor unit, $\overline{47}$ shows the indoor unit outlet and expansion element inlet (liquid line), $\overline{78}$ indicates the throttling in the expansion valve, $\overline{89}$ shows the heat absorption in the outdoor unit, and $\overline{91}$ indicates the outdoor unit outlet and compressor inlet (suction line). P-h and T-s graphs were drawn in the REFPROP 9.1 program [34]. Graphs were established using data obtained from the experimental system at the specified points. In AHP systems with R134a and R1234yf refrigerants, limited heat loss and heat gain depend on the pipe lengths in the liquid line and suction line, respectively. However, with the activation of SLHX in the AHP system with R1234yf, more heat loss and heat gain were observed in the liquid and suction lines, respectively. It was found that with the use of SLHX in the AHP system with R1234yf, the compressor inlet and outlet temperatures increased by approximately 6.5 and 3.3 °C compared to the AHP system with R1234yf. It was found that the compressor pressure ratios of the AHP system with R1234yf and the AHP system with R1234yf added SLHX were 8.12 and 7.82, respectively. This situation caused the R1234yf AHP system with SLHX to have less compressor power than the AHP system with R1234yf, as seen in Fig. 6.

6. Conclusion

This study investigated the experimental performance of an AHP system where the refrigerant flow of the AAC system was reversed, excluding the compressor. Furthermore, the impact of using a heat exchanger located between the suction and liquid lines on system performance was investigated. R134a and R1234yf refrigerants were employed in the experimental AHP system. The performance of the AHP system with R134a, R1234yf, and R1234yf with SLHX were compared. The comparisons were conducted at 1000 and 2000 rpm compressor speeds and 1.4, 2.4, and 3.2 m s^{-1} indoor unit airflow velocities. Thus, the performance comparisons of the AHP system with R134a, R1234yf and R1234yf with SLHX were made for different compressor speeds as well as different indoor unit airflow velocities.

The AHP system with R1234yf demonstrated reduced indoor unit airflow outlet temperature, heating capacity and discharge temperature in comparison to the AHP system using R134a [26,28]. Nevertheless, it was noted that the addition of the SLHX in the AHP system using R1234yf resulted in a convergence of the indoor unit airflow outlet temperature, heating capacity and discharge temperature towards that of the R134a system. It was also understood that achieving the best possible modification of the airflow rate in the interior unit was crucial for maintaining thermal comfort in the vehicle cabin. In the AHP system using R1234yf and R1234yf with SLHX, the refrigerant mass flow rate was 22.6 % and 21.7 % greater, respectively, compared to the AHP system using R134a. The compression power of the AHP system with R134a, R1234yf, and R1234yf with SLHX was in the ranges of 0.55–0.97 kW, 0.54–0.91 kW, and 0.53–0.87 kW, respectively. The COP increased by 5.9 % with the addition of SLHX to the R1234yf AHP system. The AHP system utilizing R1234yf and R1234yf with SLHX exhibited a 20.1 % and 22.2 % increase in the total exergy destruction per unit heating capacity, respectively, when compared to the R134a AHP system. The increase in the indoor unit airflow velocity increased the COP, refrigerant mass flow rate, and heating capacity, and decreased the indoor unit air outlet temperature, compressor discharge temperature, and total exergy destruction per unit heat capacity.

These findings show that cabin thermal comfort can be improved by adding an SLHX to R1234yf AHP systems, which is used as an alternative to R134a to provide thermal comfort, especially in electric vehicles, which are becoming increasingly popular, and by adjusting the indoor unit air flow rate optimally. In addition, this study has shown that adding an SLHX to the suction line of the R1234yf AHP system partially improves the heating capacity, COP and compressor outlet temperature. Moreover, it has been revealed that adjusting the indoor unit air flow rate optimally depending on the conditions and desired comfort conditions of the AHP system is important in terms of providing cabin thermal comfort and increasing system efficiency.

In future studies, the effects of using an SLHX for an AHP system using R1234ze(E) and CO_2 can be investigated. Moreover, the effect of changing indoor air flow speed on an AHP system employing a variable-capacity compressor can be studied. By using artificial intelligence technologies, indispensable in our age, the best compressor speed, indoor and outdoor unit airflow speed optimization models can be investigated according to the conditions to provide the best thermal comfort inside the vehicle cabin.

CRediT authorship contribution statement

Alpaslan Alkan: Writing – review & editing, Writing – original draft, Supervision, Investigation, Data curation, Conceptualization.

Declaration of competing interest

The author declares that they have no known competing financial interests or personal relationships that could have appeared to influence the work reported in this paper.

References

[1] Montreal protocol on substances that deplete the Ozone layer final act 1987, J. Environ. Law 1 (1) (1989) 128–136, https://doi.org/10.1093/jel/1.1.128.
[2] Y. Lee, D. Jung, A brief performance comparison of R1234yf and R134a in a bench tester for automobile applications, Appl. Therm. Eng. 35 (1) (2012) 240–242, https://doi.org/10.1016/j.applthermaleng.2011.09.004.
[3] Regulation - 517/2014 - EN - EUR-lex [Online]. Available: https://eur-lex.europa.eu/legal-content/EN/TXT/?uri=celex%3A32014R0517. (Accessed 1 March 2024).
[4] Z. Zhang, J. Wang, X. Feng, L. Chang, Y. Chen, X. Wang, The solutions to electric vehicle air conditioning systems: a review, Renew. Sustain. Energy Rev. 91 (2018) 443–463, https://doi.org/10.1016/j.rser.2018.04.005.
[5] Y. Ma, Z. Liu, H. Tian, A review of transcritical carbon dioxide heat pump and refrigeration cycles, Energy 55 (2013) 156–172, https://doi.org/10.1016/j.energy.2013.03.030.
[6] Hodnebrog, Global warming potentials and radiative efficiencies of halocarbons and related compounds: a comprehensive review, Rev. Geophys. 51 (2) (Jun. 2013) 300–378, https://doi.org/10.1002/rog.20013.
[7] C. Zilio, J.S. Brown, G. Schiochet, A. Cavallini, The refrigerant R1234yf in air conditioning systems, Energy 36 (10) (2011) 6110–6120, https://doi.org/10.1016/j.energy.2011.08.002.
[8] S. Daviran, A. Kasaeian, S. Golzari, O. Mahian, S. Nasirivatan, S. Wongwises, A comparative study on the performance of HFO-1234yf and HFC-134a as an alternative in automotive air conditioning systems, Appl. Therm. Eng. 110 (2017) 1091–1100, https://doi.org/10.1016/j.applthermaleng.2016.09.034.
[9] S. Golzari, A. Kasaeian, S. Daviran, O. Mahian, S. Wongwises, A.Z. Sahin, Second law analysis of an automotive air conditioning system using HFO-1234yf, an environmentally friendly refrigerant, Int. J. Refrig. 73 (2017) 134–143, https://doi.org/10.1016/j.ijrefrig.2016.09.009.
[10] Z. Meng, H. Zhang, M. Lei, Y. Qin, J. Qiu, Performance of low GWP R1234yf/R134a mixture as a replacement for R134a in automotive air conditioning systems, Int. J. Heat Mass Transf. 116 (2018) 362–370, https://doi.org/10.1016/j.ijheatmasstransfer.2017.09.049.
[[11]] A. Alkan, A. Kolip, M. Hosoz, Energetic and exergetic performance comparison of an experimental automotive air conditioning system using refrigerants R1234yf and R134a, J. Therm. Eng. 7 (5) (Jul. 2021) 1163–1173, https://doi.org/10.18186/thermal.978014.
[12] M.Z. Sharif, W.H. Azmi, M.F. Ghazali, M. Samykano, H.M. Ali, Performance improvement strategies of R1234yf in vapor compression refrigeration system as a R134a replacement: a review, J. Taiwan Inst. Chem. Eng. 148 (2023) 1876, https://doi.org/10.1016/j.jtice.2023.105032, 1070.
[13] H. Cho, C. Park, Experimental investigation of performance and exergy analysis of automotive air conditioning systems using refrigerant R1234yf at various compressor speeds, Appl. Therm. Eng. 101 (2016) 30–37, https://doi.org/10.1016/j.applthermaleng.2016.01.153.
[14] R. Prabakaran, D.M. Lal, S. Devotta, Effect of thermostatic expansion valve tuning on the performance enhancement and environmental impact of a mobile air conditioning system, J. Therm. Anal. Calorim. 143 (1) (2021) 335–350, https://doi.org/10.1007/s10973-019-09224-2.
[15] R. Prabakaran, D. Mohan Lal, S.C. Kim, Thermodynamic analysis of air conditioning system for a passenger vehicle with suction line heat exchanger using HFO-1234yf, Heat Transf. Eng. 45 (10) (2024) 814–832, https://doi.org/10.1080/01457632.2023.2227801.
[16] U. Gungor, M. Hosoz, Performance comparison of a mobile air conditioning system using an orifice tube as an expansion device for R1234yf and R134a, Sci. Technol. Built Environ. (2024), https://doi.org/10.1080/23744731.2024.2309124.
[17] C.C. Wang, System performance of R-1234yf refrigerant in air-conditioning and heat pump system - an overview of current status, Appl. Therm. Eng. 73 (2) (2014) 1412–1420, https://doi.org/10.1016/j.applthermaleng.2014.08.012.
[18] M. Hosoz, M. Direk, Performance evaluation of an integrated automotive air conditioning and heat pump system, Energy Convers. Manag. 47 (5) (2006) 545–559, https://doi.org/10.1016/j.enconman.2005.05.004.
[19] M. Hosoz, et al., Performance evaluation of an R134a automotive heat pump system for various heat sources in comparison with baseline heating system, Appl. Therm. Eng. 78 (2015) 419–427, https://doi.org/10.1016/j.applthermaleng.2014.12.072.
[20] Z. Wang, M. Wei, F. Peng, H. Liu, C. Guo, G. Tian, Experimental evaluation of an integrated electric vehicle AC/HP system operating with R134a and R407C, Appl. Therm. Eng. 100 (2016) 1179–1188, https://doi.org/10.1016/j.applthermaleng.2016.02.064.
[21] D. Wang, B. Yu, J. Hu, L. Chen, J. Shi, J. Chen, Caractéristiques des performances de chauffage d'un système de pompe à chaleur au CO2 pour un véhicule électrique dans un climat froid, Int. J. Refrig. 85 (2018) 27–41, https://doi.org/10.1016/j.ijrefrig.2017.09.009.
[22] H. Zou, G. Huang, S. Shao, X. Zhang, C. Tian, X. Zhang, Experimental study on heating performance of an R1234yf heat pump system for electric cars, in: Energy Procedia, 2017, pp. 1015–1021, https://doi.org/10.1016/j.egypro.2017.12.348.
[23] D. Wang, B. Yu, W. Li, J. Shi, J. Chen, Heating performance evaluation of a CO2 heat pump system for an electrical vehicle at cold ambient temperatures, Appl. Therm. Eng. 142 (2018) 656–664, https://doi.org/10.1016/j.applthermaleng.2018.07.062.
[24] M. Direk, F. Yüksel, Comparative experimental evaluation on heating performance of a mobile air conditioning system using R134a, R1234ze(E), R152A and R444A, Isi Bilim. Ve Tek. Dergisi/J. Therm. Sci. Technol. 39 (1) (2019) 31–38.
[25] K. Zhang, M. Li, C. Yang, Z. Shao, L. Wang, Exergy analysis of electric vehicle heat pump air conditioning system with battery thermal management system, J. Therm. Sci. 29 (2) (2020) 408–422, https://doi.org/10.1007/s11630-019-1128-2.
[26] M. Direk, F. Yüksel, Experimental evaluation of an automotive heat pump system with R1234yf as an alternative to R134a, Arab. J. Sci. Eng. 45 (2) (Feb. 2020) 719–728, https://doi.org/10.1007/s13369-019-04140-x.
[27] M.C. Aral, M. Suhermanto, M. Hosoz, Performance evaluation of an automotive air conditioning and heat pump system using R1234yf and R134a, Sci. Technol. Built Environ. 27 (1) (Jan. 2021) 44–60, https://doi.org/10.1080/23744731.2020.1776067.
[28] A. Alkan, A. Kolip, M. Hosoz, Experimental energy and exergy performance of an automotive heat pump using R1234yf, J. Therm. Anal. Calorim. 146 (2) (2021) 787–799, https://doi.org/10.1007/s10973-020-10035-z.
[29] Y. Huang, X. Wu, J. Jing, Research on the electric vehicle heat pump air conditioning system based on R290 refrigerant, Energy Rep. 8 (2022) 447–455, https://doi.org/10.1016/j.egyr.2022.05.112.
[30] S. Lei, B. Guo, Z. Zhao, Exergy analysis of heat pump air conditioning systems for pure electric vehicle use with low-GWP refrigerants, Int. J. Refrig. 156 (Dec. 2023) 266–277, https://doi.org/10.1016/j.ijrefrig.2023.10.009.
[31] J. Song, et al., Study on the refrigerant interchangeability under extreme operating conditions of R1234yf heat pump systems for electric vehicles, Appl. Therm. Eng. 245 (2024), https://doi.org/10.1016/j.applthermaleng.2024.122789.
[32] E. Tasdemirci, E. Alptekin, M. Hosoz, Comparative performance of an automobile heat pump system with an internal heat exchanger using R1234yf and R134a, Int. J. Exergy 33 (1) (2020) 98–113, https://doi.org/10.1504/IJEX.2020.109625.
[33] P. Arora, G. Seshadri, A.K. Tyagi, Fourth-generation refrigerant: HFO 1234yf, Curr. Sci. 115 (8) (2018) 1497–1503, https://doi.org/10.18520/cs/v115/i8/1497-1503.
[34] E.W. Lemmon, M.L. Huber, M.O. McLinden, NIST standard reference database 23: reference fluid thermodynamic and transport properties (REFPROP), version 9.0, Phys. Chem. Prop (2010) [Online]. Available: https://www.nist.gov/publications/nist-standard-reference-database-23-reference-fluid-thermodynamic-and-transport. (Accessed 11 March 2024).
[35] H. Cho, H. Lee, C. Park, Performance characteristics of an automobile air conditioning system with internal heat exchanger using refrigerant R1234yf, Appl. Therm. Eng. 61 (2) (2013) 563–569, https://doi.org/10.1016/j.applthermaleng.2013.08.030.
[36] V. Kumar, M.N. Karimi, S.K. Kamboj, Comparative analysis of cascade refrigeration system based on energy and exergy using different refrigerant pairs, J. Therm. Eng. 6 (1) (2020) 106–116, https://doi.org/10.18186/THERMAL.671652.
[37] M.J. Moran, H.N. Shapiro, Fundamentals of Engineering Thermodynamics, John Wiley and Sons, West Sussex, UK, 2006.
[38] O. Ozgener, A. Hepbasli, Modeling and performance evaluation of ground source (geothermal) heat pump systems, Energy Build. 39 (1) (2007) 66–75, https://doi.org/10.1016/j.enbuild.2006.04.019.
[39] R.J. Moffat, Describing the uncertainties in experimental results, Exp. Therm. Fluid Sci. 1 (1) (Jan. 1988) 3–17, https://doi.org/10.1016/0894-1777(88)90043-X.